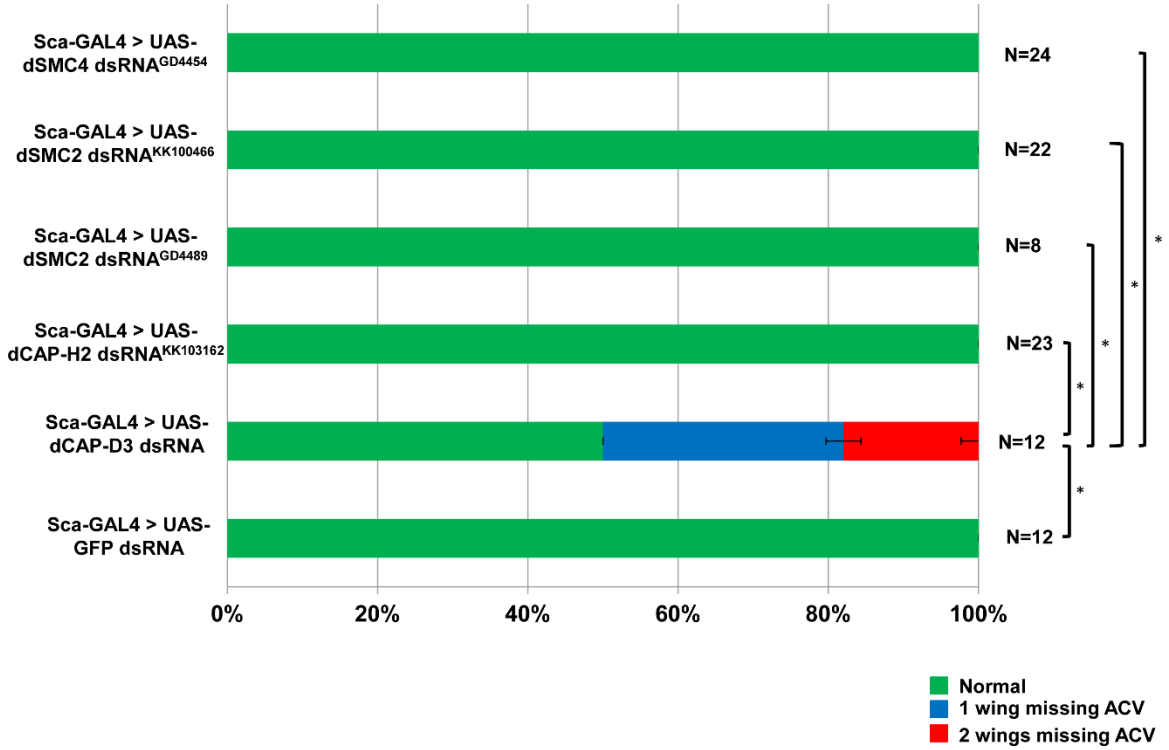

Supplementary Figure 1. Frequencies of wings per adult fly that exhibit loss (complete and partial combined) of the ACV due to sca-GAL4 driven expression of Condensin II subunits. Control flies expressing GFP dsRNA and flies expressing dCAP-D3 dsRNA are compared to flies expressing various dsRNAs against dSMC4, dSMC2, and dCAP-H2. Green bar indicates percentage of flies exhibiting normal ACV formation, blue bar indicates percentage of flies possessing 1 wing missing an ACV, and red bar indicates percentage of flies possessing 2 wings missing an ACV. Percentages were the averages of two crosses with N total flies; these experiments were performed at the same time as those depicted in Figure 1B. **$p<0.05$ (Fisher's exact t-test), in comparison to flies expressing dCAP-D3 dsRNA alone.

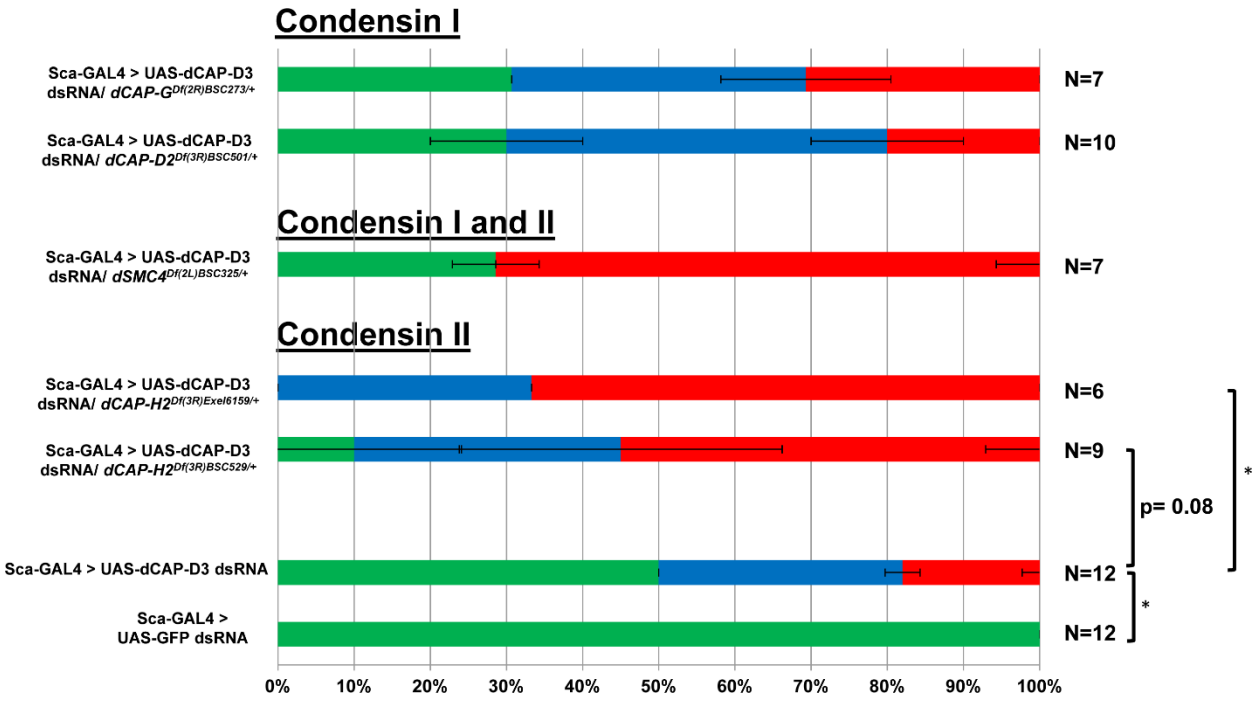

Supplementary Figure 2. Frequencies of ACV loss in flies expressing dCAP-D3 dsRNA in the background of Condensin II or Condensin I subunit haploinsufficiency. Green bar indicates percentage of flies exhibiting normal ACV formation, blue bar indicates percentage of flies possessing 1 wing missing an ACV, and red bar indicates percentage of flies possessing 2 wings missing an ACV. Percentages were the averages of two crosses with N total flies; these experiments were performed at the same time as those depicted in Figure 1B. *$p<0.05$ (Fisher's exact t-test), in comparison to flies expressing dCAP-D3 dsRNA alone.

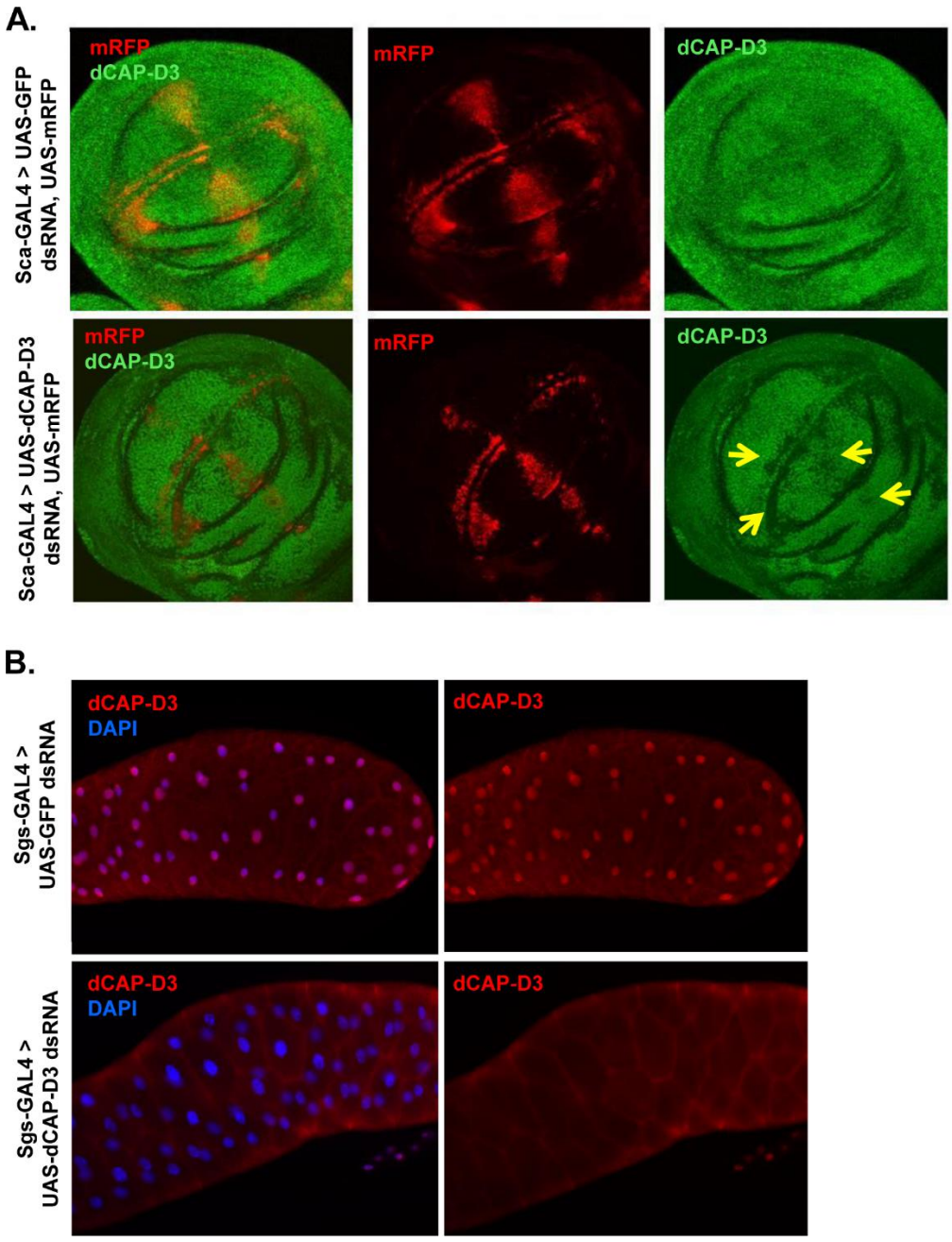

Supplementary Figure 3. dCAP-D3 protein expression is efficiently decreased by expression of dCAP-D3 dsRNA^{GD913} *in vivo*. A) Immunostaining for dCAP-D3 (green) in the pouch region of third instar larval wing discs expressing mRFP to mark cells in which sca-GAL4 drives expression. Discs expressing dCAP-D3 dsRNA show decreased staining in areas expressing mRFP (bottom row) as compared to control wing discs expressing GFP-dsRNA (top row). B) Immunostaining for dCAP-D3 (red) in third instar larval salivary glands expressing GFP or dCAP-D3 dsRNA under the control of the sgs-GAL4 driver. DAPI stained nuclei are shown in blue.

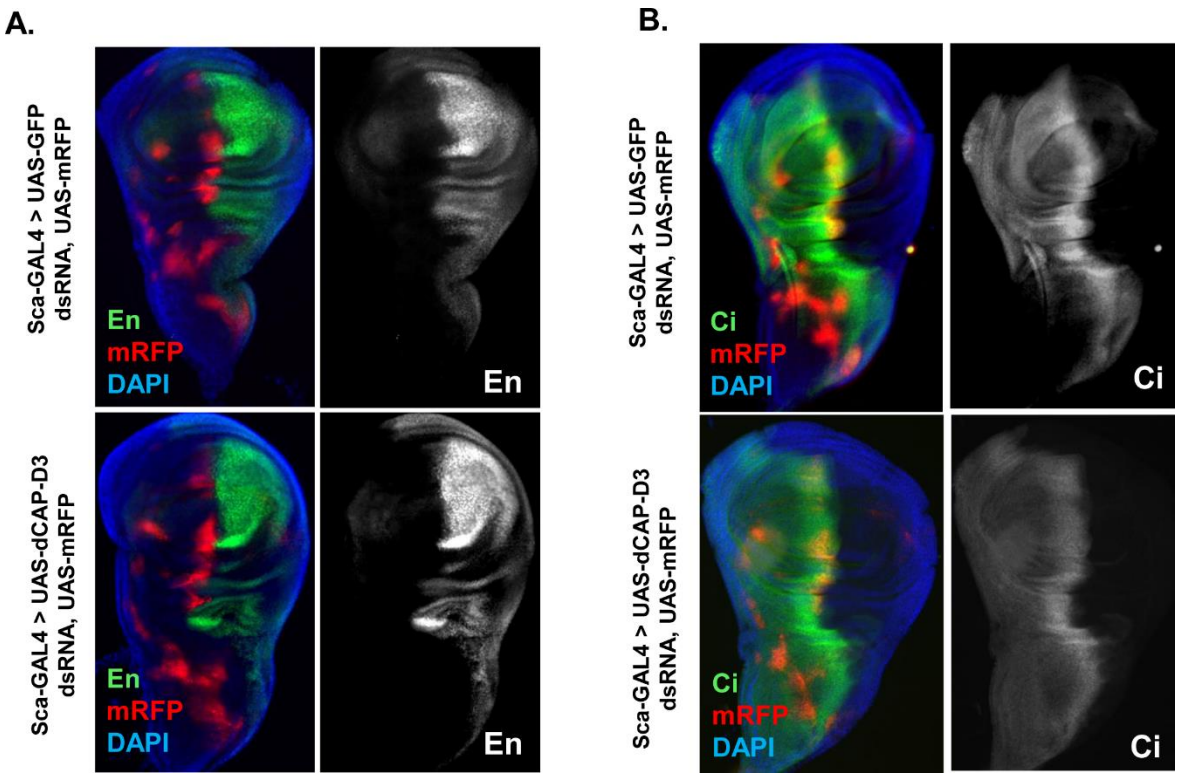

Supplementary Figure 4. dCAP-D3 deficiency in cells anterior to the A/P boundary does not compromise staining patterns of proteins at the boundary. Immunostaining for A) Engrailed (En) or B) Cubitus Interruptus (Ci), both in green, was performed in discs expressing sca-GAL4 driven GFP dsRNA (top row) or dCAP-D3 dsRNA (bottom row). Myristolated Red Fluorescent Protein (mRFP) was expressed to mark cells in which sca-GAL4 is active. Immunostaining was performed twice on at least 5 individual larvae per experiment.

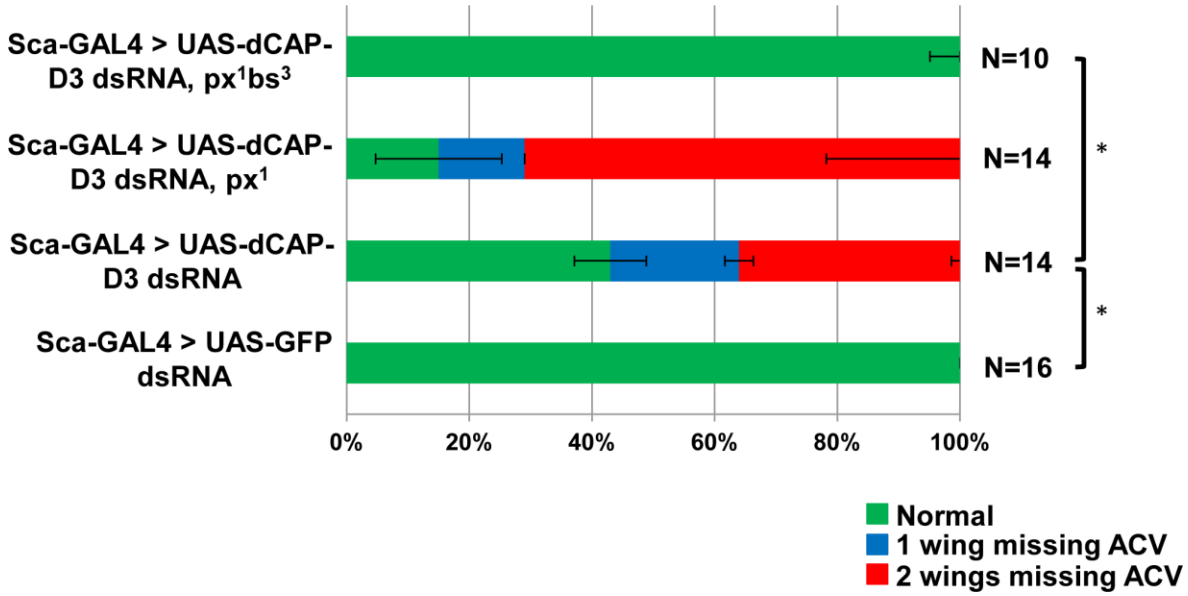

Supplementary Figure 5. Frequencies of ACV loss in flies expressing dCAP-D3 dsRNA and a dSRF mutant allele. The dSRF mutant allele also contains a mutation in the px allele, and therefore, frequencies of ACV loss in flies expressing dCAP-D3 dsRNA and the px mutant allele, alone, are also presented. Green bar indicates percentage of flies exhibiting normal ACV formation, blue bar indicates percentage of flies possessing 1 wing missing an ACV, and red bar indicates percentage of flies possessing 2 wings missing an ACV. Percentages were the averages of two crosses with N total flies. *$p<0.05$ (Fisher's exact t-test), in comparison to flies expressing dCAP-D3 dsRNA alone.

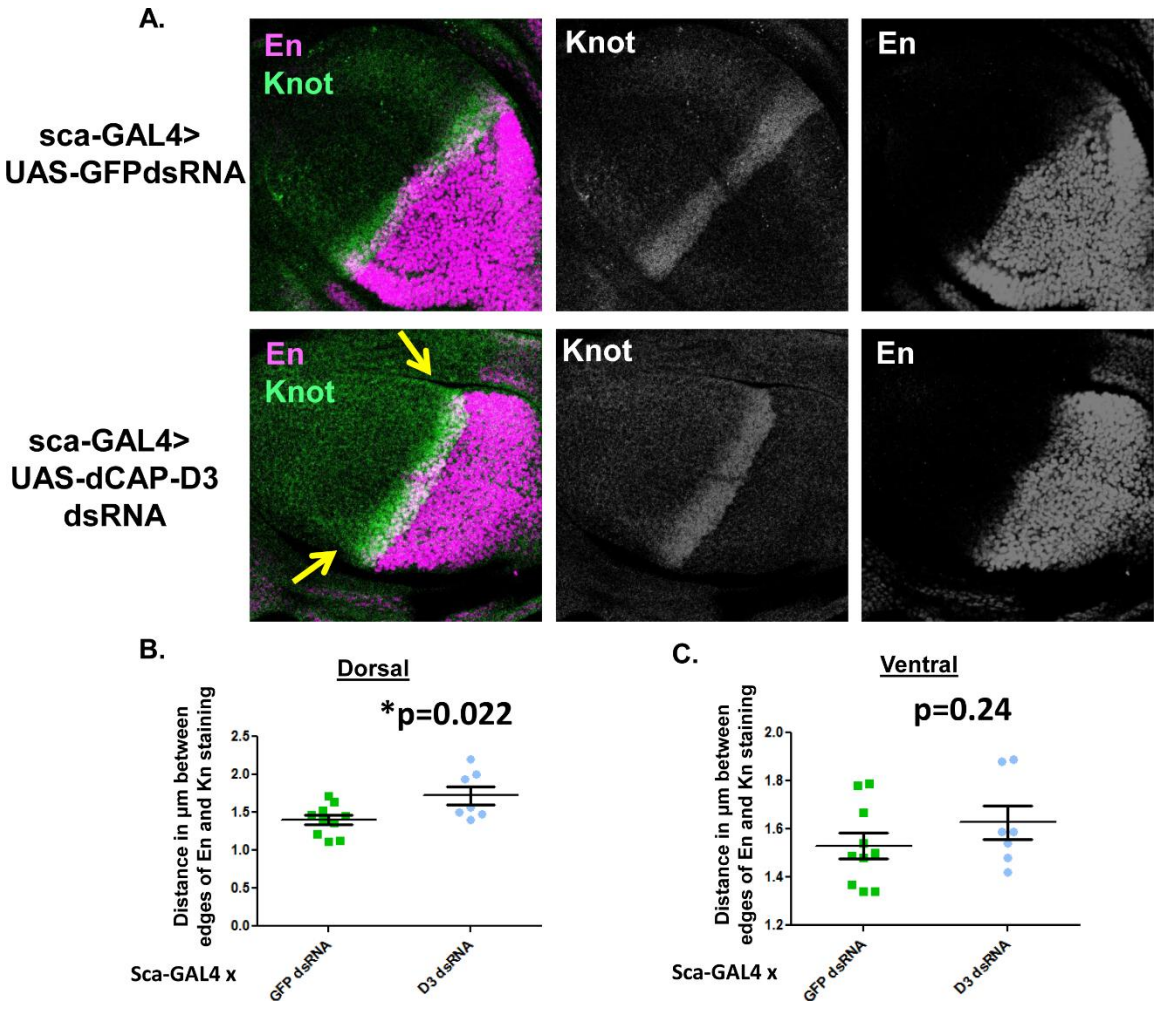

Supplementary Figure 6. Knot expression extends further from the posterior border in dCAP-D3 dsRNA expressing wing discs. A) Immunostaining for Knot (green) and En (pink) demonstrates a wider band of Knot staining from the posterior border, as marked by En expression, in sca-GAL4 driven dCAP-D3 dsRNA expressing wing discs. Quantitation of the distance in µM between the edges of En and Knot in GFP dsRNA expressing (green dots) or dCAP-D3 dsRNA expressing (blue dots) wing discs is shown for the dorsal (B) and ventral (C) halves of the discs. Statistics were calculated using the student's unpaired T-test.

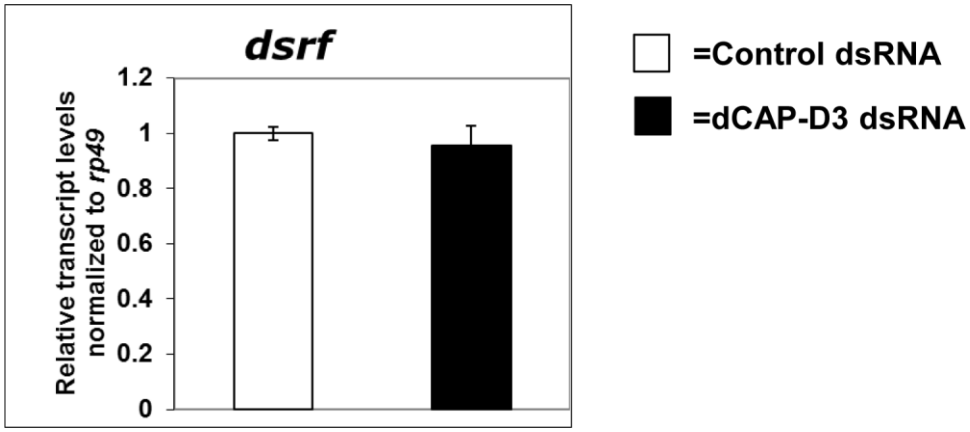

Supplementary Figure 7. dCAP-D3 deficiency does not affect *dsrf* transcript levels in S2 cells. qRT-PCR for levels of *dsrf* transcripts in S2 cells shows that dCAP-D3 dsRNA treatment (black bars) does not change the levels of *dsrf* transcripts in comparison to treatment with Control (T7) dsRNA (white bars). Data is the average of three experiments.

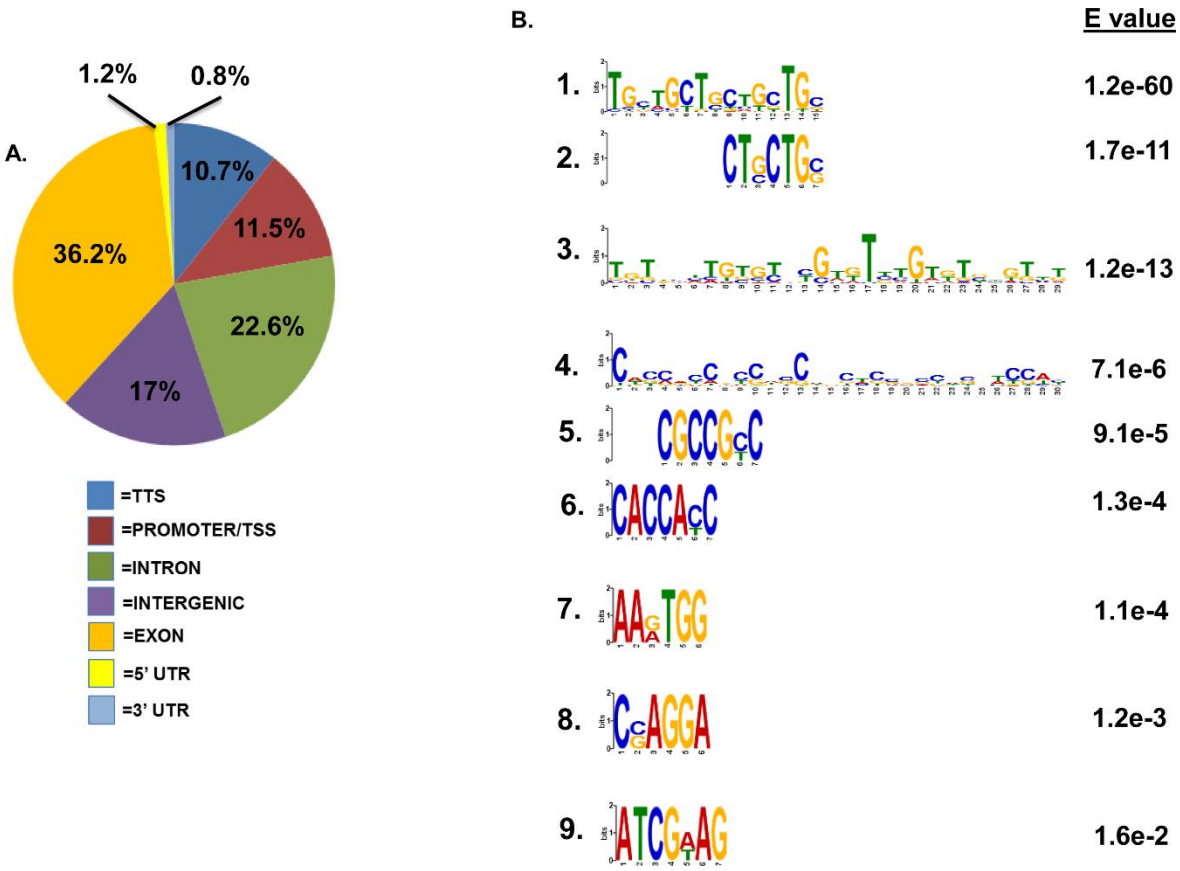

Supplementary Figure 8. Analysis of dCAP-D3 binding sites. A) Pie chart showing the percentage of dCAP-D3 binding sites (as identified by ChIP-seq) that are located in different genomic regions. B) The top 1000 dCAP-D3 binding sites that fell outside of promoters were analyzed for common sequence motifs. The sequences of the nine motifs identified to be significant are shown along with their corresponding E values.

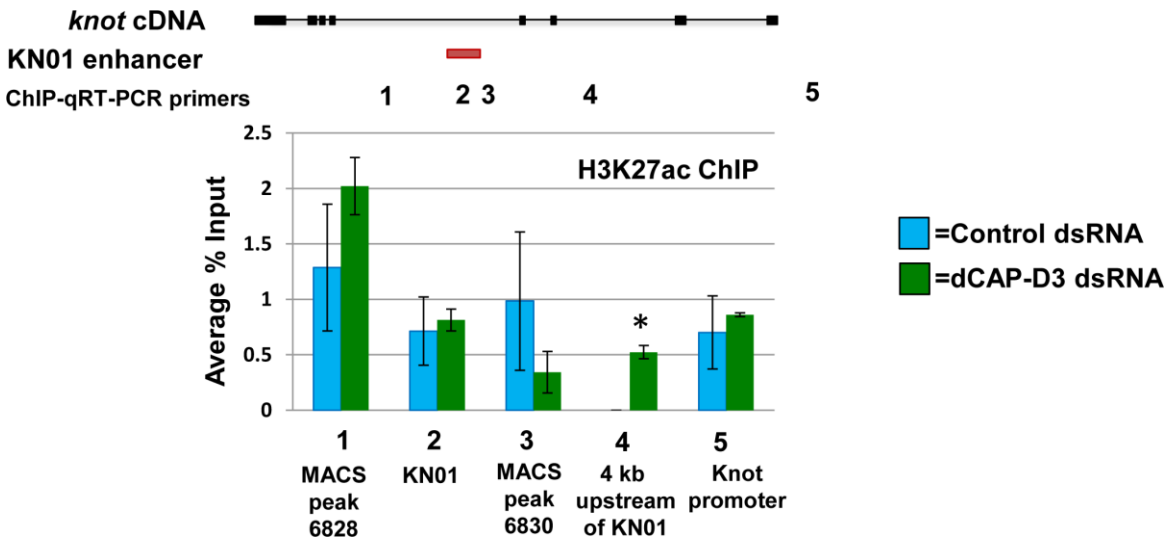

Supplementary Figure 9. Distribution of Histone H3 acetylated at lysine 27 does not change in dCAP-D3 deficient cells. ChIP for Histone H3 acetylated at lysine 27 (H3K27) was performed in S2 cells treated with control (blue bars) or dCAP-D3 dsRNA (green bars) and analyzed by qRT-PCR. The relative location of the KN01 enhancer is depicted by a red box. Location of sequences targeted by primer sets for the ChIP-qRT-PCR experiments are shown below the diagram of the *knot* cDNA (numbers 1-5). *$p<0.05$ (student's unpaired t-test).

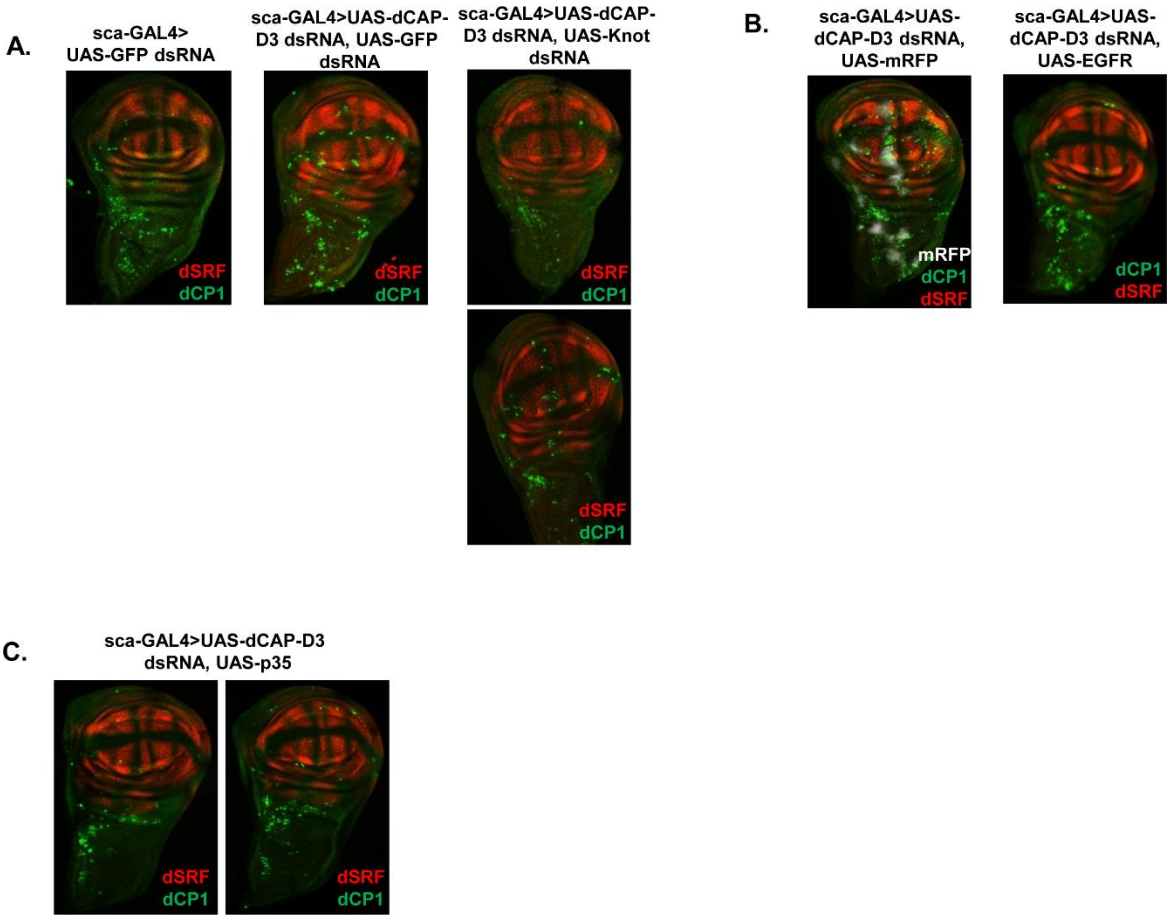

Supplementary Figure 10. Whole disc images of experiments in Figure 6. A-C) Experiments are identical to those described in Figure 6, but pictures allow for visualization of dCP1 staining of the notum, which does not change significantly between the different genotypes.

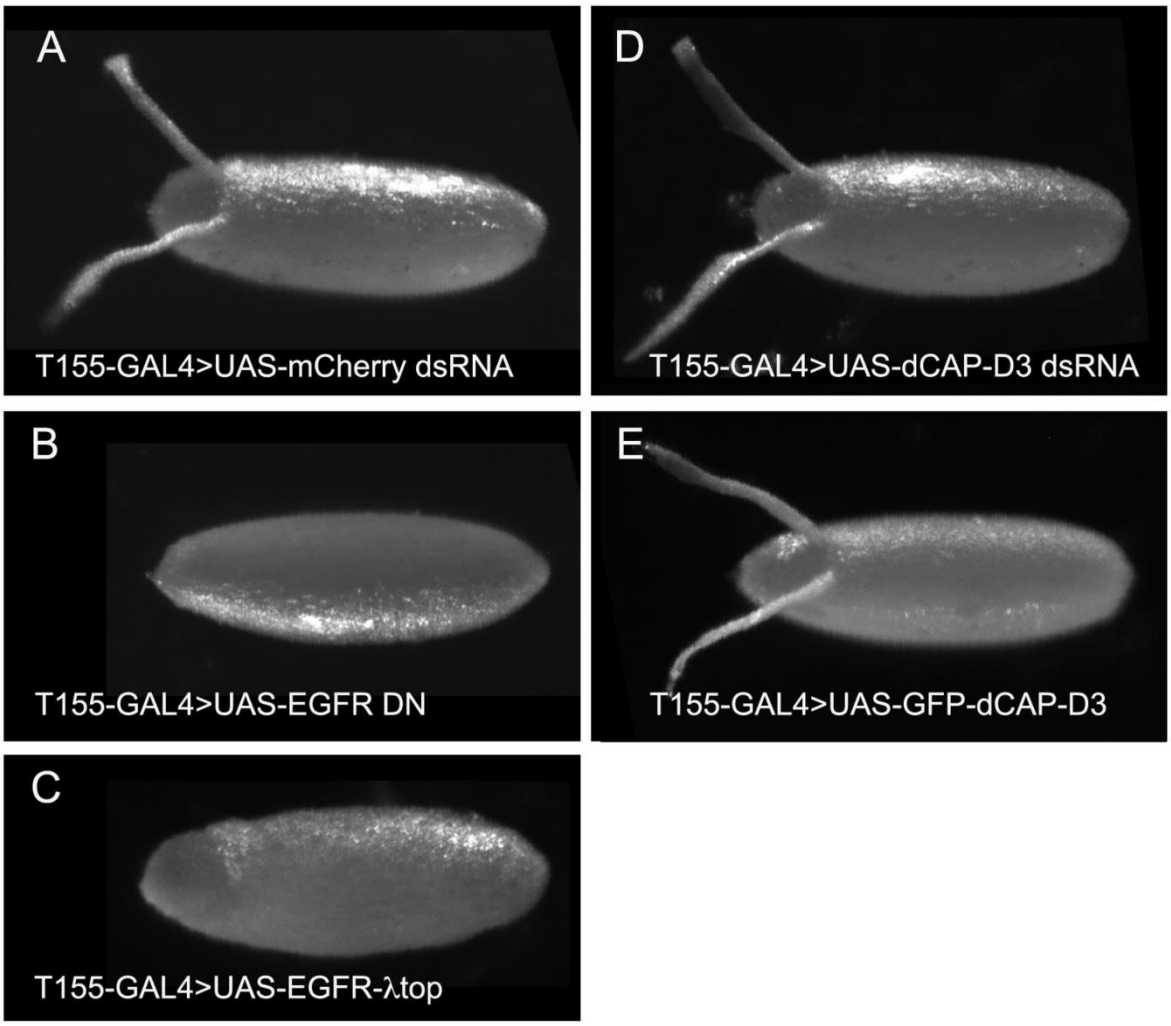

Supplemental Figure 11. Neither dCAP-D3 dsRNA nor UAS-GFP-dCAP-D3 expression in follicle cells disrupts dorsal appendage formation in the egg. The indicated UAS transgenes were driven by the ubiquitous follicle cell driver T155-GAL4 in females at 27˚C for at least 2 days. Eggs were collected and photographed on agar plates using a Leica M165 FC Stereomicroscope. A) Control egg expressing mCherry dsRNA. The dorsal appendages, found on the dorsal-anterior side of the eggshell, are normal. B) Egg expressing EGFR DN. The dorsal appendages are lost due to the eggshell becoming ventralized. C) Egg expressing activated EGFR (UAS-EGFR-λtop) in which the eggshell is dorsalized. Ectopic dorsal midline material, likely the operculum, replaces the dorsal appendages when EGFR is strongly activated. D) Egg expressing dCAP-D3 dsRNA. No dorsal appendage defects are observed. E) Egg overexpressing GFP-dCAP-D3. No dorsal appendage defects are observed.

Supplementary Materials and Methods

Antibodies and dilutions used in immunofluorescence experiments

Primary antibodies included YZ384-dCAP-D3 (Longworth et al., 2012) at 1:100, anti-dSRF (gift from Dr. Seth Blair) at 1:500, anti-knot (Jinushi-Nakao et al., 2007) at 1:1000, anti-engrailed (DSHB) at 1:50, anti-CI (DSHB) at 1:10, anti-DCP1 (Cell Signaling) at 1:400 and anti-dpERK (Cell Signaling) at 1:200. Secondary antibodies used were: Alexa-Fluor donkey anti-rabbit 488 (Life Technologies, A21206), Alexa-Fluor goat anti-mouse 488 (Life Technologies, A11001), Alexa-Fluor goat anti-mouse568 (Life Technologies, A11004), Alexa-Fluor goat anti-mouse 647 (Life Technologies, A21235), Alexa-Fluor highly cross absorbed goat anti-guinea pig 488 (Life Technologies, A11073) and Alexa-Fluor goat anti-rat (Life Technologies, A11006).

Primers

qRT-PCR primers:

Knot F1: GAGATAATCCTCAAGAGGGCTGCC

Knot R1: GGAGCCATCCTGGACACTGAC

dSRF F1: GCATTCGACGCACTCGCACATG

dSRF R1: CTTCGTGTATTCACTCGGTCGAG

dCAP-D3 F3: CGTGCTGTTGCTTTACTTCGGCC

dCAP-D3 R3: GGCGCATGATGAAGAGCATATCCTG

Primers used for making dsRNAs:

uniD3dsRNA#1F: CTAATACGACTCACTATAGGGAGTGCAGATTACGTGCTGGAAGC

uniD3dsRNA#1R: CAGGGGATTGACTAGGACCAG

Data analysis of ChIP-seq results

Reads were trimmed of adapters and low-quality bases with Trim Galore (v.0.3.7 using cutadapt v.1.8, http://www.bioinformatics.babraham.ac.uk/projects/trim_galore/) in paired-end mode using default

parameters. FastQC (v.0.11.3, http://www.bioinformatics.bbsrc.ac.uk/projects/fastqc) was used to verify the quality of trimmed samples. Reads were aligned to BDGPr6 (from the Flybase FB2015_01 release, 24 February 2015) with bowtie (Langmead et al., 2009) (v.1.0.0, -m 1 --best --strata) and filtered to retain only properly paired alignments. Peaks were identified using MACS2 (v.2.0.9 20111102) (Zhang et al., 2008) with default settings except for an explicit shift size estimated from 100,000 properly paired alignments (--shiftsize=125 --nomodel). Peaks were annotated using Homer (Heinz et al., 2010)(v3.12, 6-8-2012) with the same genome assembly and annotations as above (r6.04) with the modification that non-intergenic peak distances were calculated to the nearest transcript rather than to the nearest transcription start site (TSS). Peak regions were divided into promoter-proximal (TSS -1kb to +100bp) and enhancer categories. For each class, the top 1,000 peaks by MACS2 score were used for motif analysis using the MEME-ChIP (Machanick and Bailey, 2011) web server (v.4.10, http://meme.ebi.edu.au/meme/doc/meme-chip.html) with default settings and "All Drosophila" motifs. The E-value is an estimate of the expected number of motifs with the given log likelihood ratio (or higher), and with the same width and number of occurrences, that one would find in a similarly sized set of random sequences.

References

HEINZ, S., BENNER, C., SPANN, N., BERTOLINO, E., LIN, Y. C., LASLO, P., CHENG, J. X., MURRE, C., SINGH, H. & GLASS, C. K. 2010. Simple combinations of lineage-determining transcription factors prime cis-regulatory elements required for macrophage and B cell identities. *Mol Cell,* 38**,** 576-89.

JINUSHI-NAKAO, S., ARVIND, R., AMIKURA, R., KINAMERI, E., LIU, A. W. & MOORE, A. W. 2007. Knot/Collier and cut control different aspects of dendrite cytoskeleton and synergize to define final arbor shape. *Neuron,* 56**,** 963-78.

LANGMEAD, B., TRAPNELL, C., POP, M. & SALZBERG, S. L. 2009. Ultrafast and memory-efficient alignment of short DNA sequences to the human genome. *Genome Biol,* 10**,** R25.

LONGWORTH, M. S., WALKER, J. A., ANDERSSEN, E., MOON, N. S., GLADDEN, A., HECK, M. M., RAMASWAMY, S. & DYSON, N. J. 2012. A shared role for RBF1 and dCAP-D3 in the regulation of transcription with consequences for innate immunity. *PLoS Genet,* 8**,** e1002618.

MACHANICK, P. & BAILEY, T. L. 2011. MEME-ChIP: motif analysis of large DNA datasets. *Bioinformatics,* 27**,** 1696-7.

ZHANG, Y., LIU, T., MEYER, C. A., EECKHOUTE, J., JOHNSON, D. S., BERNSTEIN, B. E., NUSBAUM, C., MYERS, R. M., BROWN, M., LI, W. & LIU, X. S. 2008. Model-based analysis of ChIP-Seq (MACS). *Genome Biol,* 9**,** R137.